EFFECTS OF TEMPERATURE AND VELOCITY GRADIENTS ON DOPPLER WIDTHS

A. PERAIAH and B. A. VARGHESE

Indian Institute of Astrophysics, Bangalore, India

(Received 6 May, 1986)

Abstract. We have investigated how the gradients of temperature and expansion velocities will change the emergent profiles from an extended medium in spherical symmetry. Variation of the source function and expansion velocities are assumed. The following variations of temperature are employed:

(1) $T(r) = T_0$ (isothermal case),

(2) $T(r) = T_0(r/r_0)^{1/2}$,

(3) $T(r) = T_0(r/r_0)^{-1}$,

(4) $T(r) = T_0(r/r_0)^{-2}$,

(5) $T(r) = T_0(r/r_0)^{-3}$.

The profiles calculated present an interesting feature of broadening.

1. Introduction

It is customary to compute theoretical profiles by employing a profile function which does not incorporate the temperature gradients. The source function takes into account the temperature gradients (see Athay, 1972). A temperature and frequency-dependent source function is employed in many cases, assuming that the profile of the line remains unchanged through the medium. When the temperature changes continuously the Doppler width also changes. Therefore, one must take into consideration these changes when evaluating the emergent profiles. The effects become more pronounced when the medium is in motion. In the next section we will introduce temperature variation in a Doppler profile and calculate the emergent profiles of lines in different media.

2. Brief description of the Procedure of Calculation and Discussion of the Results

We employ the Doppler profile function given (see Rybicki, 1970) by

$$\phi(x, \pm v(r)) = \frac{1}{\delta(r)\sqrt{\pi}}\, e^{-(x \pm v(r)\mu)^2/\delta^2(r)}, \tag{1}$$

where

$$x = \frac{\nu - \nu_0}{\Delta_D}, \tag{2}$$

Astrophysics and Space Science **126** (1986) 295–300.

$$\Delta_D = \frac{v_0}{CV}, \qquad V = \left(\frac{2kT}{m}\right)^{1/2}, \tag{3}$$

$$v(r) = v_{gas}(r)/V_{therm}, \tag{4}$$

$$\delta(r) = \frac{V_{therm}(r)}{V_{th}}, \tag{5}$$

$$V_{therm}(r) = \left[\frac{2kT(r)}{m}\right]^{1/2}. \tag{6}$$

The temperature changes are introduced into the profile through the quantity $\delta(r)$. In the foregoing equations v_0 and v stand for the frequencies in the line centre and at any other point. $V(r)$ is the velocity of the gas measured in terms of mean thermal velocity. Δ_D is the Doppler width, and V is the mean thermal velocity at T. V_{th} is the average or a constant mean thermal velocity. We will employ the profile function defined in

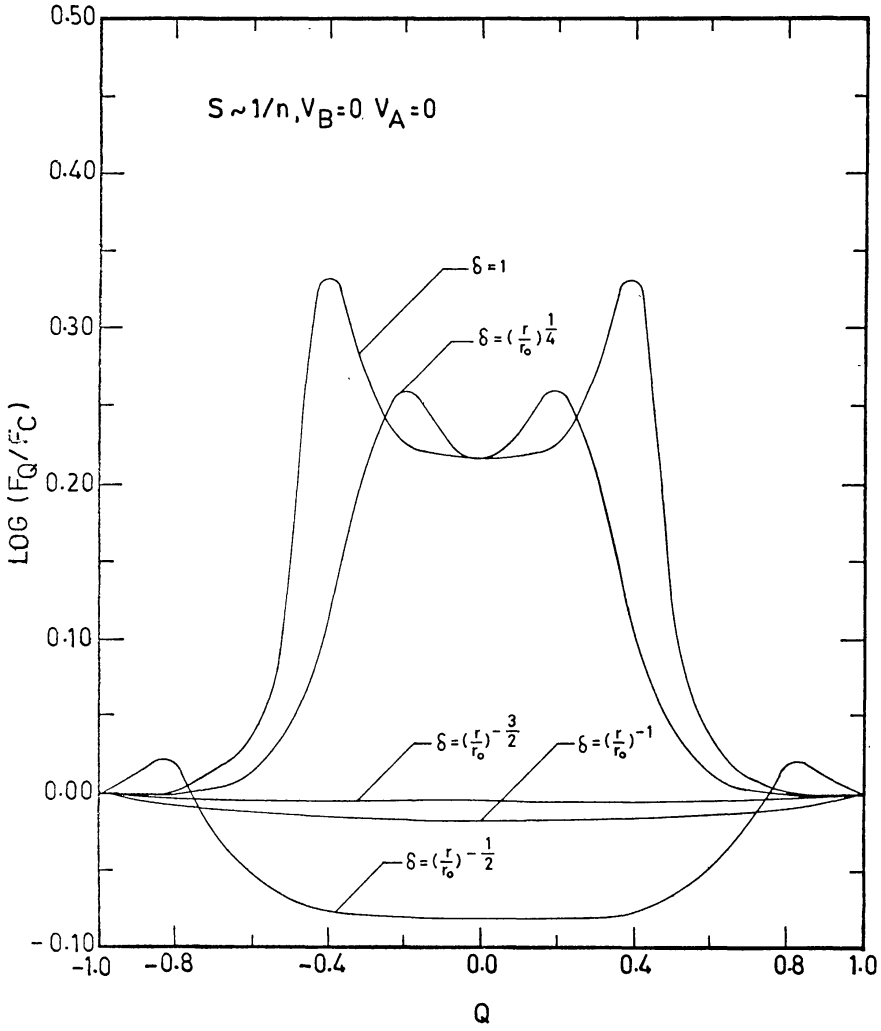

Fig. 1. Profiles without velocity gradients for $S \sim 1/n$.

Equation (1) and calculate the emergent line profile in the line-of-sight. We have assumed a spherically-symmetric media around a centrally-emitting source. We have specified the variation of the source function as well as velocity changes along the radius. The inner radius is taken to be 10^{12} cm and the outer radius to be 10^{13} cm. The total radial optical depth is of the order of 1000.

We have assumed the following variations of temperature:

$$T(r) = T_0 \quad \text{(isothermal medium)}, \tag{7}$$

$$T(r) = T_0(r/r_0)^{1/2}, \tag{8}$$

$$T(r) = T_0(r/r_0)^{-1}, \tag{9}$$

$$T(r) = T_0(r/r_0)^{-2}, \tag{10}$$

$$T(r) = T_0(r/r_0)^{-3}. \tag{11}$$

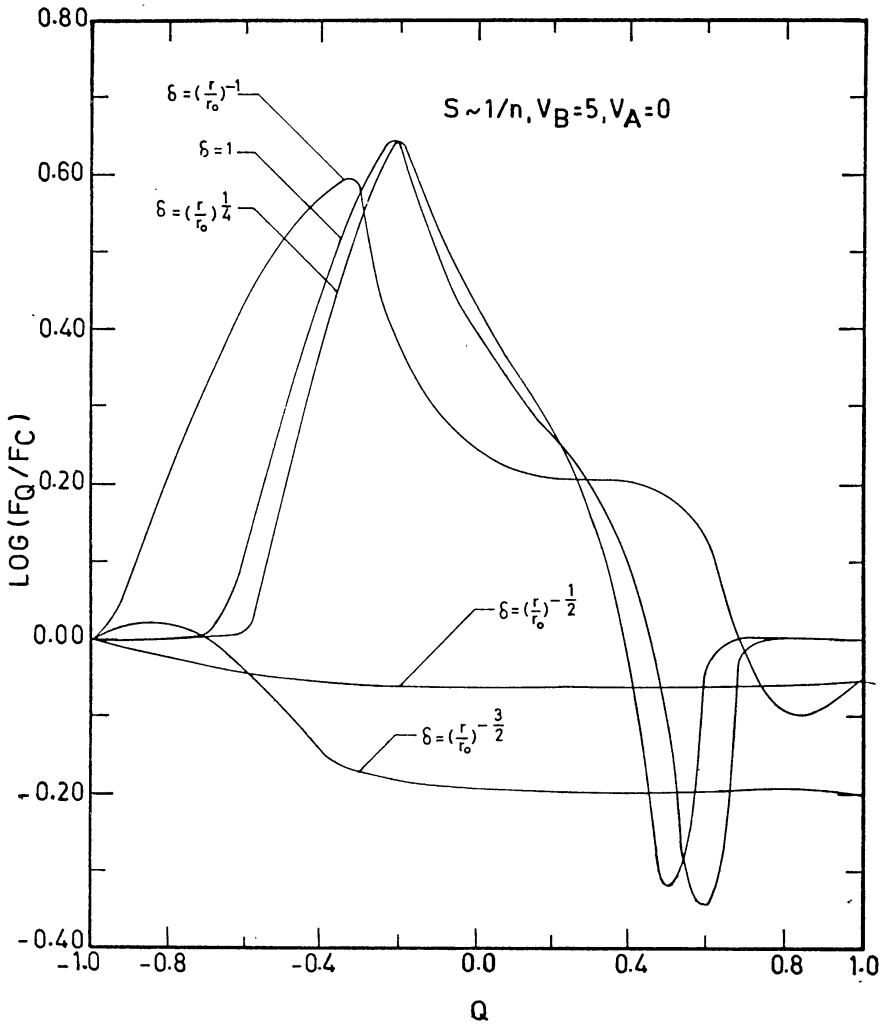

Fig. 2. Profiles with velocity gradients for $S \sim 1/n$.

If Equations (7) to (11) are substituted in Equation (5) we successively obtain,

$$\delta(r) = 1\,, \tag{12}$$

$$\delta(r) = (r/r_0)^{1/4}\,, \tag{13}$$

$$\delta(r) = (r/r_0)^{-1/2}\,, \tag{14}$$

$$\delta(r) = (r/r_0)^{-1}\,, \tag{15}$$

$$\delta(r) = (r/r_0)^{-3/2}\,. \tag{16}$$

The radial dependence of $\delta(r)$ in Equations (12) to (16) is utilized when the profile function $\phi[(x, v(r)]$ is evaluated at different radial points. We divided the entire spherical shell into 60 subshells and let the source function vary as $1/n$ and $1/n^2$ where n is the number of the shell, $n = 1$ corresponds to the innermost shell, and $n = 60$ to the outermost shell. The method of calculation of the flux is described in Peraiah (1980).

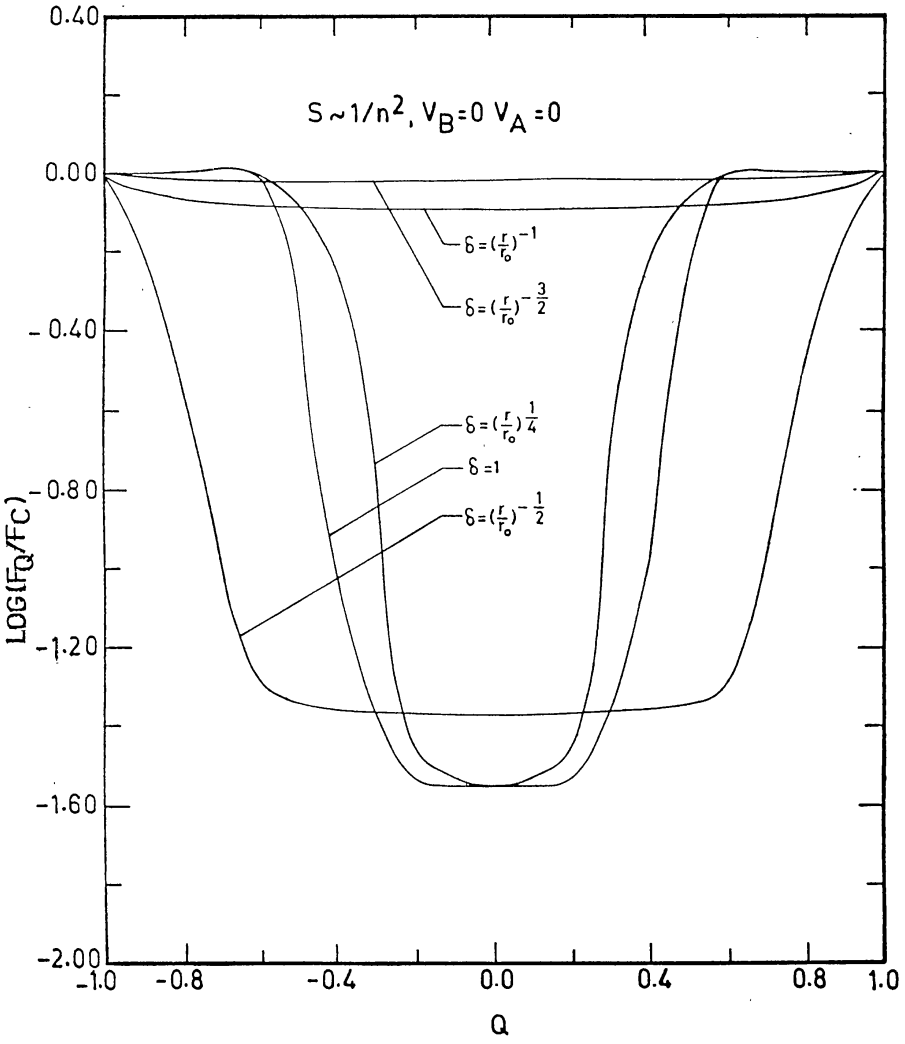

Fig. 3. Profiles without velocity gradients for $S \sim 1/n^2$.

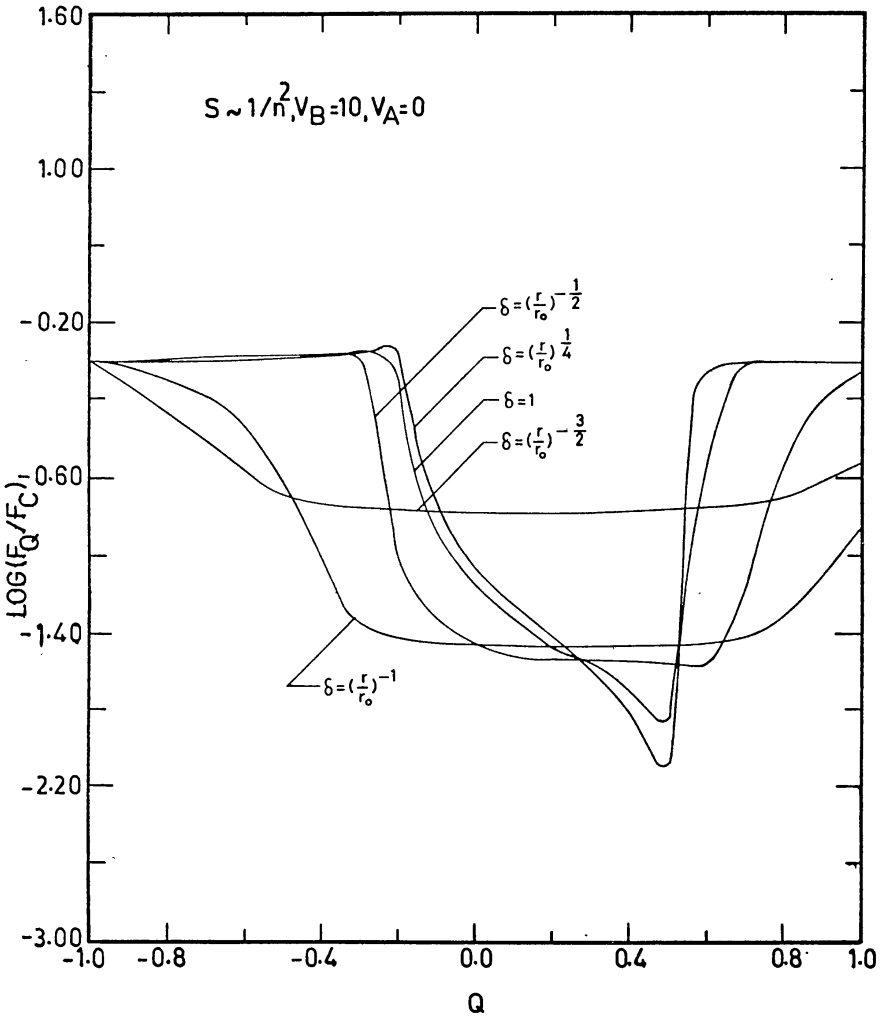

Fig. 4. Profiles with velocity gradients for $S \sim 1/n^2$.

The profiles are described in Figures 1 through 4. We have plotted $\log(F_Q/F_C)$ versus Q where Q is defined as

$$Q = \frac{X_Q}{|X_{\max}|}\,, \tag{17}$$

where X_q is the normalized frequency at any point in the line (as defined in Equation (2)) and $X_{\max}$ is the maximum value of X. When $X_q = \pm X_{\max}$, $Q = \pm 1$. Thus we normalize all the profiles irrespective of the expansion velocities. In each of the figures we plotted the emergent profiles corresponding to the values of $\delta(r)$ given in Equations (12)–(16).

In Figure 1, we set $S \sim 1/n$ and $V_A = V_B = 0$ where V_A and V_B correspond to the velocities (in mean thermal units) at $A(\tau = \tau_{\max})$ and $B(\tau = 0)$. We find that the profiles corresponding to $\delta = 1$ (isothermal case) produce emission with self-absorption. A similar profile is obtained for $\delta(r) = (r/r_0)^{1/4}$ for which the temperature changes as $r^{1/2}$, which has a smaller emission than the former. However, the profiles for $T \sim r^{-1}, r^{-2}$,

r^{-3} do not show any emission and instead appear in absorption. We introduced velocity gradients and plotted these profiles in Figure 2. These profiles show a P Cygni tendency, i.e., red emission and blue absorption. However, the profile corresponding to $\delta(r) = (r/r_0)^{-1}$ $(T(r) \sim r^{-2})$ shows the P cygni characteristics clearly when velocity gradients are present, while it shows weak, but broadened, absorption when velocity gradients are absent. This is the combined effect of the temperature and velocity gradients on the profiles. The profile corresponding to $\delta = (r/r_0)^{-3/2}(T(r) \sim r^{-3})$ also shows a little red emission but the line profile is not completely shown here because the frequency grid points are not enough for the full line to develop.

In Figure 3, we considered a radiation field described by $S \sim 1/n^2$. This corresponds to a very dilute radiation compared to the previous case. Those results are described in Figures 1 and 2. The profiles corresponding to $\delta = (r/r_0)^{-1}$ and $(r/r_0)^{-3/2}$ exhibit the same characteristics, i.e., very broad, weak absorption lines like those in Figure 1. This fact shows that the density of the radiation field does not change the profile characteristics when $T(r) \sim r^{-2}$ and r^{-3}. However, we obtain deep and broad absorption profiles when $\delta = 1$, $(r/r_0)^{1/4}$ and $(r/r_0)^{-1/2}$ (i.e., $T(r) =$ constant, $T(r) \sim r^{1/2}$, and r^{-1}). In Figure 4, we plot profiles that have both velocity and temperature gradients. All the lines appear in absorption and the lines for $\delta = (r/r_0)^{-1}$ and $(r/r_0)^{-3/2}$ become particularly prominent with the introduction of velocity gradients. These profiles were not so prominent in Figure 3. Profiles for $\delta = 1$ and $(r/r_0)^{1/4}$ exhibit a sharp rise on the violet side.

References

Athay, G.: 1972, *Radiation Transport in Spectral Lines*, D. Reidel Publ. Co., Dordrecht, Holland.
Peraiah, A.: 1980, *J. Astrophys. Astron.* **1**, 17.
Rybicki, G.: 1970, in *Spectrum Formation in Stars with Steady-State Extended Atmospheres*, NBS Special Publ., No. 332.